Different orientation of the transition dipole moments of two similar Pt(II) complexes and their potential for high efficiency organic light-emitting diodes

Christian Mayr, Masatsugu Taneda, Chihaya Adachi, Wolfgang Brütting

Angaben zur Veröffentlichung / Publication details:

Mayr, Christian, Masatsugu Taneda, Chihaya Adachi, and Wolfgang Brütting. 2014. "Different orientation of the transition dipole moments of two similar Pt(II) complexes and their potential for high efficiency organic light-emitting diodes." *Organic Electronics* 15 (11): 3031–37. https://doi.org/10.1016/j.orgel.2014.07.042.

Organic Electronics, 15 (2014) 3031-3037 https://doi.org/10.1016/j.orgel.2014.07.042

Different orientation of the transition dipole moments of two similar Pt(II) complexes and their potential for high efficiency organic light-emitting diodes

Christian Mayr,[1]* Masatsugu Taneda,[2] Chihaya Adachi,[2,3]** and Wolfgang Brütting[1]***

[1] *Institute of Physics, University of Augsburg, Universitätsstraße 1, 86159 Augsburg, Germany*
[2] *Center for Organic Photonics and Electronics Research (OPERA), Kyushu University, 744 Motooka, Nishi, Fukuoka 819-0395, Japan*
[3] *International Institute for Carbon Neutral Energy Research, Kyushu University, 744 Motooka, Nishi, Fukuoka 819-0395, Japan*

*E-mail: Christian.Mayr@physik.uni-augsburg.de

**E-mail: adachi@cstf.kyushu-u.ac.jp

***E-mail: Wolfgang.Bruetting@physik.uni-augsburg.de

Abstract

The efficiency of organic light-emitting diodes (OLEDs) is especially limited by their low light outcoupling efficiency. An approach for its enhancement is the use of horizontally oriented emitter molecules with respect to the substrate. In this study we quantitatively determine the orientation of the optical transition dipole moments in doped films of two similar phosphorescent Pt(II) complexes having a linear molecular structure. These emitters are employed in OLED devices and their efficiency is analyzed by optical simulations. For an OLED with slightly more horizontally oriented emitter molecules an external quantum efficiency (η_{EQE}) of 15.8% at low current-density is realized, indicating a relative improvement of outcoupling efficiency of 5.3% compared to the isotropic case. However, a very similar complex adopting isotropic molecular orientation yields η_{EQE} of only 11.5% implying an imperfect charge carrier balance in the OLED device and a shift of the recombination zone. Furthermore, we highlight the enormous potential of horizontal molecular orientation of emitting molecules in OLEDs.

Keywords: Organic light-emitting diode, Molecular orientation, Platinum(II) complex, Light outcoupling, Optical simulation

1. Introduction

Since the pioneering work of Tang and VanSlyke [1], organic light-emitting diodes (OLEDs) have been investigated for over 20 years and have been recently introduced to the market for mass production. This technology used in displays for mobile phones, televisions or lighting applications is getting more and more widespread offering many advantages to already established technologies: brilliant colours, angle-independent viewing characteristics, the possibility to design transparent light sources or the deployment on flexible substrates etc. In times of scarce resources, OLEDs can also be used for lighting applications where established technologies with point light sources (LEDs) can be replaced by area-light-sources.

Tremendous effort has been made to enhance the efficiency of OLEDs. An important value characterizing the efficiency is the external quantum efficiency η_{EQE} [2]:

$$\eta_{EQE} = \gamma \cdot \eta_r \cdot q_{eff} \cdot \eta_{out} . \qquad (1)$$

In this equation γ is the charge carrier balance, η_r is the radiative exciton fraction, q_{eff} is the effective radiative quantum efficiency, which results from the intrinsic radiative quantum efficiency q by a modification in the OLED cavity due to the Purcell effect [3], and η_{out} is the light outcoupling efficiency. By a precise adjustment of the transport layers - especially by using doped transport layers - the charge carrier balance γ can be brought to unity [4,5]. The radiative exciton fraction η_r is limited to 25% for fluorescent emitters due to spin-statistics [6,7]. However by the introduction of phosphorescent emitters, which facilitate spin-orbit coupling and harvest both singlet and triplet excitons, the radiative exciton fraction η_r becomes 100% [8-10]. Especially transition metals like Platinum [8,11] or Iridium [5,12,13] are good candidates to form metal-organic phosphorescent emitters and have been extensively investigated in the past. By optimizing the charge-balance ratio γ, the use of phosphorescent emitters having an (effective) radiative quantum efficiency q_{eff} near unity, internal quantum efficiencies of almost 100% can be realized [5]. However, the remaining factor - the outcoupling efficiency η_{out} - is especially limiting the efficiency due to the refractive index mismatch of

the organic layers and the substrate, resulting in substrate and waveguide modes; but also near-field coupling to surface plasmons (SPs) at the interface of the organic and the cathode decreases the overall outcoupling efficiency [3]. Thus, the ultimate challenge to further increase the efficiency of OLEDs is to enhance the light outcoupling efficiency. Even though there are approaches in order to overcome these challenges by using macroextractors, patterned substrates or the concept of index-coupling [14], these methods require extra efforts during production, change emission characteristics, are non-trivial to fabricate and are overall expensive. Especially the molecular orientation of the transition dipole moments with respect to the substrate has a huge effect on the coupling to SPs. Whereas molecules which have their transition dipole moments oriented perpendicular to the substrate couple strongly to SPs, horizontally oriented ones show suppressed coupling [15,16]. A general value of ~20% outcoupling efficiency has been assumed for a long time [17], but by optical simulations and experiments it has been shown that this value can be increased to over 30% by using oriented phosphorescent Ir(III) complexes as the emitter [18-20]. Consequently a new approach for increasing the outcoupling efficiency is to use the intrinsic property of some emitters to orient in neat and doped films [21]. Besides, it should also be noted that other beneficial effects like increased mobility of charge carriers are accompanied with molecular orientation [22].

In neat films it has been shown by Yokoyama et al. that horizontal molecular orientation is especially found in linear-shaped molecules. The longer the molecular chain, the higher the anisotropy becomes [21]. Based on this design concept, we report about two Pt(II) complexes which have been modified in a way to promote horizontal orientation: using a ligand with a rod-like structure. Compared to Ir(III) complexes, which exhibit an octahedral structure, Pt(II) complexes could be promising candidates to study orientation phenomena due to their square-planar structure. Recently, Pt(II) complexes have been reported to achieve comparable quantum efficiencies close to *fac*-tris(2-phenylpyridine)iridium (III) [$Ir(ppy)_3$] and OLED devices with η_{EQE} >20% have been fabricated [23-26].

We quantitatively determine the orientation of the transition dipole moments in doped films of two similar Pt(II) emitters. Employing these emitters in OLED-devices, an efficiency analysis taking the

molecular orientation into account is performed. Finally, we give an outlook about the potential of horizontally oriented Pt(II) complexes for high-efficiency OLED devices.

2. Experimental

For this study two similar Pt(II) complexes have been synthesized (Fig. 1): Platinum (II) (2-phenyl-5-(4''-(4'''-tert-butylphenyl)phenyl)pyridinato-*N*,*C'')(2,4-pentanedionato-O*,*O)* (**1Pt**) [27] and platinum (II) (2-phenyl-5-(4''-(4''-phenylphenyl)pyridinato-*N*,*C'')(2,4-pentanedionato-O*,*O)* (**2Pt**) (see Supplementary Information for the details of the synthesis). The difference of both molecules is the missing butyl group on the linear ligand of **2Pt**.

All substrates have been cleaned upon sonication in pure water, acetone, boiling in 2-propanol and subsequent ultraviolet ozone treatment.

In Fig. 1 the stack layout of the studied OLEDs, the molecular structures of the used materials and the highest occupied molecular orbital (HOMO) and lowest unoccupied molecular orbital (LUMO) levels are shown. The device consists of a glass substrate, 100 nm indium tin-oxide (ITO), 40 nm *N,N′*-Di-[(1-naphthyl)-*N,N′*-diphenyl]-1,1′-biphenyl)-4,4′-diamine (NPD) as the hole transport layer (HTL), 10 nm 1,3-Bis(N-carbazolyl)benzene (mCP) as the electron blocking layer (EBL), 20 nm mCP doped with 6 wt.% **1Pt** or **2Pt** as the emission layer (EML), 10 nm 2,9-dimethyl-4,7-diphenyl-1,10-phenanthroline (BCP) as the hole blocking layer (HBL), 40 nm tris(8-hydroxyquinoline)aluminium (Alq_3) and a cathode of 100 nm Mg:Ag (20:1) and 20 nm Ag. The 10 nm of neat mCP as EBL are also needed for the exciton confinement in the EML due to its high triplet energy (T_1=2.9 eV) compared to NPD (T_1=2.29 eV) [28]. It prevents energy transfer from the emitter to the triplet state of the HTL NPD [29,30].

The HOMO of the emitters was determined by photoemission yield measurement (AC-3, Riken Keiki Co. Ltd.) and the LUMO level was calculated by subtracting the HOMO-LUMO gap which was estimated from the absorption edge in the UV-Vis absorption spectrum from the HOMO level.

All organic layers were deposited in a vacuum of $< 2 \times 10^{-4}$ Pa at an evaporation rate of 0.1 nm/s, except for the emitter, which was deposited at a rate of 0.06-0.1 nm/s. The substrates were rotated at equivalent positions from the axis during deposition. The active area of the OLEDs was circularly

shaped with a diameter of 1 mm.

The current density-voltage-luminance characteristics were measured using a semiconductor parameter analyzer (4155C, Agilent Technologies Inc.) connected to a silicon photodiode (1835-C, Newport Co.). The electroluminescent (EL) spectra of the OLEDs were measured using a multichannel spectrometer (SD 2000, Ocean Optics). The η_{EQE} was calculated from the current-density, luminance and EL spectrum.

The photoluminescence (PL) quantum yield of the phosphorescence (Φ_{PL}) was measured on 50 nm doped films of 6 wt.% **1Pt** or **2Pt** in mCP on fused silica substrates using an absolute PL quantum yield measurement system (Quantaurus-QY, C11347, Hamamatsu Photonics) at an excitation wavelength of 337 nm. The PL emission spectra were measured using a JASCO FP-6000 spectrometer at room temperature showing a very similar emission with a peak emission at 547 nm and 544 nm for the films containing **1Pt** and **2Pt**, respectively (Fig. 2).

To determine the molecular orientation in doped films, angular-dependent photoluminescence measurements have been performed [31]. The samples consisted of glass substrates with 15 nm mCP doped with 6 wt.% **1Pt** or **2Pt** and encapsulated by a glass slide. The samples were attached to a fused silica half cylinder prism by index matching liquid and the emission angle was changed by the use of a rotation stage. The spectra were measured using a fibre optical spectrometer (SMS-500, Sphere Optics) and a polarizing filter to distinguish between p- and s-polarized light. The excitation of the samples was performed with a 375 nm cw laser diode with a fixed excitation angle of 45°.

3. Results and Discussion

3.1 Determination of the orientation of the transition dipole moment

It has been shown by Yokoyama et al. that there is a relationship between molecular structure and orientation in neat films. With increasing molecular length the anisotropy in the film also increases [21]. Based on this concept two phosphorescent Pt(II) complexes **1Pt** and **2Pt** have been synthesized incorporating a rod-like ligand in order to promote horizontal molecular orientation also in doped films.

There are two established methods to quantitatively measure molecular orientation of amorphous organic films: variable-angle spectroscopic ellipsometry (VASE) [21] and measurements of the angular dependent emission profile of films [16,31] or entire OLED stacks [18,32,33]. VASE is applied to neat films but lacks sensitivity measuring the molecular orientation of the dopant in guest:host systems. Measurements of the angular dependent emission profile of OLED devices (with a special ETL-thickness) and emission layers are performed by EL and by PL excitation, respectively.

Both methods - VASE and measurements of the angular dependent emission characteristics - yield information about the orientation of the transition dipole moments by measuring absorption and emission, respectively. Because VASE is not sensitive enough to measure the molecular orientation in doped films, edge-emission measurements for **1Pt** have been performed showing qualitatively a more horizontal molecular orientation [27]. However, for a quantitative analysis angular dependent measurements of the emission profile need to be conducted. With this method the p-polarized PL emission (considered in the *x*-*z*-plane, see inset of Fig. 3) is compared to optical simulations of radiating dipoles in a multilayer stack [31]. Since the p-polarized emission consists of horizontally oriented p_x and vertically oriented p_z dipoles, information about the ratio of horizontal and vertical transition dipole moments can be obtained. The degree of emitter orientation can be characterized by the orientation anisotropy factor Θ, which is the fraction of vertically oriented (p_z) to the total amount of transition dipole moments (p_x, p_y, p_z). An isotropic orientation (33% p_x, 33% p_y and 33% p_z dipoles) has the same amount of horizontal p_x and vertical p_z transition dipoles, thus yielding a ratio of 1:1 and corresponds to Θ=0.33. For a complete horizontal orientation Θ=0, since there is no contribution from vertically oriented transition dipoles.

Samples of 15 nm mCP doped with 6 wt.% of **1Pt** and **2Pt** have been excited with a 375 nm laser. The angular dependent p-polarized emission spectra together with optical simulations for a completely isotropic and horizontal orientation of the transition dipole moments are displayed in Fig. S2 and S3 of the Supplementary Information. Cross-sections at a wavelength of 580 nm are shown in Fig. 3. The profile shows a sharp decrease in intensity at 41°, which can be attributed to the angle of total internal reflection at the glass/air interface. At higher angles substrate modes are outcoupled and the

intensity is especially sensitive to the degree of molecular orientation. For the dopant **1Pt** the analysis yields a ratio of the amount of radiating horizontal p_x to vertical p_z transition dipoles of 1:0.86±0.03 (thus Θ=0.86/2.86 = 0.301, corresponding to an overall of 30% vertical p_z and 70% horizontal transition dipole moments). This value indicates a slight deviation from an isotropic orientation of the transition dipole moments towards a more horizontal one. The dopant **2Pt** yields a ratio of 1:0.97±0.03 (Θ=0.327), meaning almost perfect isotropic orientation.

In contrast to the expectation, the degree of horizontal molecular orientation of the linear- and planar-shaped Pt(II) complexes is similar to Ir(III) complexes (Θ=0.33-0.23) [19,20,32,34]. Molecular structure influences the intermolecular interaction during deposition [21,36] and often allows predictions about their orientation in films. However, it is not the only factor that must be taken into account: glass transition temperature of the film, substrate temperature and surface roughness are additional parameters. The interplay of these factors defines the molecular orientation [22,35-37]. It has been shown for neat films that non-isotropic orientation especially occurs during film growth at substrate temperatures much lower than their glass transition temperature being in a kinetically controlled state [35-37]. In this temperature regime a wide range of molecular orientations can arise. However, the studied Pt(II) complexes deposited at RT, have too high kinetic energy facilitating reorganization on the surface of the film, hindering the molecules to adopt a complete horizontal orientation. Additionally, for the molecules **1Pt** and **2Pt** having a different molecular structure and thus a different potential energy at the film surface, we ascribe the different molecular orientation to a difference in the kinetic energy loss process during film growth. Molecules of **1Pt** on the surface of mCP do not have sufficient energy to migrate and undergo complete randomization as for molecules of **2Pt**. Thus, the incorporation of the butyl group is responsible for the promotion of horizontal orientation of the molecules in the doped mCP film.

3.2 OLED Efficiency Analysis

Based on the result of the difference in molecular orientation of the emitters **1Pt** and **2Pt** in an mCP host, these two dopants are employed in OLED devices and their efficiency is compared. Their

emission spectra are very similar and both emitters show a photoluminescence quantum yield Φ_{PL} of 50% in a doped mCP film (6 wt.%). Based on equation (1), we perform an efficiency analysis and focus on the quantification of the individual contributions to η_{EQE}. The knowledge of molecular orientation of the emitter molecules in the host allows for a precise calculation of the outcoupling efficiency η_{out}, leading to implications for the other factors constituting η_{EQE} [38].

The stack layout of the investigated OLED with 100 nm ITO/40 nm NPD/10 nm mCP/20 nm **1Pt** or **2Pt** in mCP (6 wt.%)/10 BCP/40 nm Alq_3/100 nm Mg:Ag (20:1)/20 nm Ag is shown in Fig. 1. Fig. 4b shows the EL spectra of the devices exhibiting a peak emission at 547 nm and 544 nm for the device with **1Pt** and **2Pt** as the emitter, respectively. No other emission from the host or transport materials was observed indicating charge carrier confinement on the dopants. The OLED with the emitter **1Pt** yields maximum η_{EQE} values of 15.8% whereas **2Pt** only yields 11.5% at a current density of 0.01 mA/cm² (Fig. 4a). The efficiency roll-off at higher current densities can likely be ascribed to triplet-triplet and triplet-polaron annihilation [39,40].

Optical simulations, calculating the dissipated power to the different optical modes (emission to air, emission to substrate, waveguides and surface plasmons) have been performed [34]. The refractive indices and thicknesses of the multilayer structure of the OLED, the emission spectrum and the fraction of horizontal to vertical radiating dipoles were taken into account. For the OLED with the oriented **1Pt** emitter, an outcoupling efficiency η_{out} of 23.7% is calculated. The assumption of an isotropic orientation only yields a value of 22.5% due to a stronger coupling to surface plasmons. Thus, by having an increased horizontal molecular orientation, this emitter achieves a relative enhancement of outcoupling efficiency by 5.3% compared to the isotropic case.

In Fig. 5 the calculated η_{EQE} with a varying ETL thickness is shown. The thickness of the ETL strongly influences the efficiency due to changing interference conditions and the microcavity environment. For the OLED stack a maximum efficiency is expected at an ETL thickness of 48 nm, confirming that the studied stack is well-optimized. Due to the use of phosphorescent emitters, a radiative exciton fraction η_r of 100% is assumed for the calculation. Microcavity effects and molecular orientation modifying the

radiative quantum efficiency [3,40] and causing differences in q_{eff} between the two OLEDs were taken into account. For the OLED with **1Pt** as the emitter the calculation of η_{EQE} yields 15.7% which corresponds very well to the measured value (see summarized values in Table 1). This perfect match can only be achieved assuming 100% charge carrier balance¥ and locating the position of the emission zone (EZ) at the interface between the dye-doped and the undoped mCP (EZ=0). This is due to the fact that the relatively high HOMO level of **1Pt** of -5.56 eV induces hole-trapping at the doped/undoped mCP interface. Moving the emission zone closer to the cathode would result in a decrease of efficiency. This possibility, however, is not supported by the high experimental value for η_{EQE}.

For the OLED device with **2Pt** as the emitter, the lower η_{EQE} value cannot be described by a difference in molecular orientation alone. We ascribe this behaviour to the lower HOMO level of -5.64 eV and LUMO level of -2.84 eV compared to **1Pt**. Due to the lower energy levels a decrease of hole- and an increase of electron-trapping on the dopant can be expected impeding exciton formation at the doped/undoped mCP interface. For the proposed mechanism a shift of the emission zone towards the BCP layer (EZ=20) can be anticipated. Even though the PL spectra of both emitters are almost identical, the EL spectra (Fig. 4b) show a significant difference especially at longer wavelengths. A change of the location of the emission zone in the OLED stack changes interference conditions modulating the EL spectrum. The calculation of the optical response (based on the OLED stack) [42] with an emission zone at the doped/undoped mCP interface (EZ=0) and at the doped mCP/BCP interface (EZ=20) is shown in Fig. 4b. The calculation shows that shorter wavelengths are enhanced and longer wavelengths supressed for EZ=20 as compared to the case with EZ=0, which is consistent to the experimental result for the **2Pt** OLED. This suggests a shift of the emission zone towards BCP. In addition to optical differences of the two OLEDs, also electrical differences are apparent. In Fig. 4c the OLED with **1Pt** as the dopant is showing higher current-densities for the same voltages compared to the device with **2Pt** suggesting a different charge-transport or charge injection into the EML, resulting in a lower charge carrier balance for the OLED with **2Pt**.

By assuming the emission zone between the doped/undoped mCP interface (EZ=0) and the doped mCP/BCP interface (EZ=20), the charge carrier balance must be decreased and confined to 75%<¥ < 86% in order to describe the experimental results properly. Even though it is not possible to measure the charge carrier balance ¥ by experimental means, the accurate knowledge of outcoupling efficiency ¦ $_{out}$ (which is highly dependent on the degree of molecular orientation) allows for a quantification of ¥ , explaining the lower-than-expected efficiency of the **2Pt** OLED.

3.3 Potential for high-efficiency OLEDs

In Fig. 6 the ¦ $_{EQE}$ for the studied OLED stack is calculated with a variation of the amount of vertical transition dipole moments p_z and the intrinsic quantum efficiency q . Assuming ideal radiative quantum efficiency and charge carrier balance of 100%, an ¦ $_{EQE}$ of 36.3% is possible by using perfectly horizontally aligned emitters without any outcoupling structures. Thus, by increasing the horizontal molecular orientation, an enhancement in efficiency of 61% is possible. By also using outcoupling structures (like macroextractors etc.) the ¦ $_{EQE}$ can even be increased up to 66.9%. Thus, there is still much space for improving the OLED efficiency: both the radiative quantum efficiency and molecular orientation have to be optimized by molecular design.

4. Conclusions

The orientation of the transition dipole moments has been measured in doped films for two similar Pt(II) complexes having a ligand with a linear structure. Only the Pt(II) complex with a butyl group attached to the linear ligand promotes horizontal molecular orientation of this molecule used as a dopant in an mCP host. The external quantum efficiency of 15.8% of the OLED comprising the oriented dopant could be successfully predicted by optical simulations taking molecular orientation into account. The emission zone could be determined to be located at the doped/undoped mCP interface. The lower efficiency of the OLED with the isotropically oriented complex with 11.5% cannot be described by the isotropic orientation of the dopant alone. Additionally an imbalance of charge carrier

recombination of 75%<¥ < 86%, accompanied by a shift of the emission zone towards BCP must be considered.

A further improvement of device efficiency up to 36.3% is possible by using highly-oriented dopants with a perfect radiative quantum efficiency highlighting the enormous potential that horizontally oriented emitters bear in them.

Supplementary Information

Supplementary data associated with this article can be found in the online version.

Acknowledgements

We acknowledge financial support by the Deutsche Forschungsgemeinschaft (DFG, contract no. Br 1728/13-1), the Bayerische Forschungsstiftung and the Japanese Society for the Promotion of Science (JSPS). This work was supported by the New Energy and Industrial Technology Development Organization (NEDO), BEANS project.

References

1. C.W. Tang, S.A. VanSlyke, Organic electroluminescent diodes, Appl. Phys. Lett. 51 (1987) 913–915.
2. T. Tsutsui, E. Aminaka, C.P. Lin, D.-U. Kim, Extended molecular design concept of molecular materials for electroluminescence: sublimed-dye films, molecularly doped polymers and polymers with chromophores, Phil. Trans. R. Soc. Lond. A 355 (1997) 801–814.
3. S. Nowy, B.C. Krummacher, J. Frischeisen, N.A. Reinke, W. Brütting, Light extraction and optical loss mechanisms in organic light-emitting diodes: Influence of the emitter quantum efficiency, J. Appl. Phys. 104 (2008) 123109.
4. M. Pfeiffer, K. Leo, X. Zhou, J.S. Huang, M Hofmann, A Werner, J. Blochwitz-Nimoth, Doped organic semiconductors: Physics and application in light emitting diodes, Org. Electron. 4 (2003) 89.
5. C. Adachi, M.A. Baldo, M.E. Thompson, S.R. Forrest, Nearly 100% internal phosphorescence efficiency in an organic light emitting device, J. Appl. Phys. 90 (2001) 5048–5051.
6. M.A. Baldo, D.F. O'Brien, M.E. Thompson, S.R. Forrest, Excitonic singlet-triplet factor in a semiconducting thin film, Phys. Rev. B 60 (1999) 14422.
7. M. Segal, M.A. Baldo, R.J. Holmes, S.R. Forrest, Z.G. Soos, Excitonic singlet-triplet ratios in molecular and polymeric organic materials, Phys. Rev. B 68 (2003) 075211.
8. M.A. Baldo, D.F. O'Brien, Y. You, A. Shoustikov, S. Sibley, M.E. Thompson, S.R. Forrest, Highly efficient phosphorescent emission from organic electroluminescent devices, Nature 395 (1998), 151.
9. J.S. Wilson, A.S. Dhoot, A.J.A.B. Seeley, M.S. Khan, A. Köhler, R.H. Friend, Spin-dependent exciton formation in π-conjugated compounds, Nature 413 (2001) 828.
10. Y. Sun, N.C. Giebink, H. Kanno, B. Ma, M.E. Thompson, S.R. Forrest, Management of singlet and triplet excitons for efficient white organic light-emitting diodes, Phys. Rev. B 60 (1999) 14422.
11. D.F. O'Brien, M.A. Baldo, M.E. Thompson, S.R. Forrest, Improved energy transfer in electrophosphorescent devices, Appl. Phys. Lett. 74, 442 (1999).
12. M.A. Baldo, S. Lamansky, P.E. Burrows, M.E. Thompson, S.R. Forrest, Very high green organic light-emitting devices based on electrophosphorescence, Appl. Phys. Lett. 75 (1999) 4.
13. S. Lamansky, P. Djurovich, D. Murphy, F. Abdel-Razzaq, H.-E. Lee, C. Adachi, P. Burrows, S.R. Forrest, M.E. Thompson, Highly phosphorescent Bis-Cyclometalated Iridium Complexes: Synthesis,

Photophysical Characterization, and Use in Organic Light Emitting Diodes, J. Am. Chem. Soc. 123 (2001) 4304-4312.

14. J. Frischeisen, B.J. Scholz, B.J. Arndt, T.D. Schmidt, R. Gehlhaar, C. Adachi, W. Brütting, Strategies for light extraction from surface plasmons in organic-light-emitting diodes, J. Photon. Energy 1(1) (2011) 011004.
15. W.H. Weber, C.F. Eagen, Energy transfer from an excited dye molecule to the surface plasmons of an adjacent metal, Opt. Lett. 4 (1979) 236–238.
16. J. Frischeisen, D. Yokoyama, A. Endo, C. Adachi, W. Brütting, Increased light outcoupling efficiency in dye-doped small molecule organic light-emitting diodes with horizontally oriented emitters, Org. Electron. 12 (2011) 809-817.
17. K. Meerholz, D.C. Müller, Outsmarting waveguide losses in thin-film light-emitting diodes, Adv. Funct. Mat. 11 (2001), 251-253.
18. M. Flämmich, J. Frischeisen, D.S. Setz, D. Michaelis, B.C. Krummacher, T.D.Schmidt, W. Brütting, N. Danz, Oriented phosphorescent emitters boost OLED efficiency, Org. Electron. 12 (2011) 1663–1668.
19. S.-Y. Kim, W.-I. Jeong, C. Mayr, Y.-S. Park, K.-H. Kim, J.-H. Lee, C.-K. Moon, W. Brütting, J.-J. Kim, Organic Light-Emitting Diodes with 30% External Quantum Efficiency Based on a Horizontally Oriented Emitter, Adv. Funct. Mater. 23 (2013) 3896–3900.
20. K.-H. Kim, C.-K. Moon, J.-H. Lee, S.-Y. Kim, J.-J. Kim, Highly Efficient Organic Light-Emitting Diodes with Phosphorescent Emitters Having High Quantum Yield and Horizontal Orientation of Transition Dipole Moments, Adv. Mater. 26 (2014), 3844-3847.
21. D. Yokoyama, A. Sakaguchi, M. Suzuki, C. Adachi, Horizontal orientation of linear-shaped organic molecules having bulky substituents in neat and doped vacuum-deposited amorphous films, Org. Electron. 10 (2009), 127-137.
22. D. Yokoyama, Y. Setoguchi, A. Sakaguchi, M. Suzuki, C. Adachi, Orientation Control of Linear-Shaped Molecules in Vacuum-Deposited Organic Amorphous Films and Its Effect on Carrier Mobilities, Adv. Funct. Mater. 20 (2010) 386–391.
23. Z.M. Hudson, C. Sun, M. G. Helander, H. Amarne, Z.-H. Lu, and S. Wang, Enhancing Phosphorescence and Electrophosphorescence Efficiency of Cyclometalated Pt(II) Compounds with Triarylboron, Adv. Funct. Mater. 20 (2010) 3426–3439.

24. Z.B. Wang, M.G. Helander, Z. M. Hudson, J. Qiu, S. Wang, Z. H. Lu, Pt(II) complex based phosphorescent organic light-emitting diodes with external quantum efficiencies above 20%, Appl. Phys. Lett. 98 (2011) 213301.

25. E. Turner, N. Bakken, J. Li, Cyclometalated Platinum Complexes with Luminescent Quantum Yields Approaching 100%, Inorganic Chemistry 52 (2013) 52, 7344-7351.

26. Y. Chi, L. Huang, G. Tu, W. Hung, Y. Song, M. Tseng, P. Chou, G.Lee. K. Wong. S. Cheng, W. Tsai, Mechanoluminescence and Efficient White-Emitting OLEDs for Pt(II) Phosphors Bearing Spatially Encumbered Pyridinyl Pyrazolate Chelates, J. Mater. Chem. C 1 (2013), 7582-7592.

27. M. Taneda, T. Yasuda, C. Adachi, Horizontal Orientation of Linear-Shaped Platinum (II) Complex in Organic Light-Emitting Diodes with a High Light Out-Coupling Efficiency, Appl. Phys. Express 4 (2011), 071602.

28. J. Lee, N. Chopra, S.H. Eom, Y. Zheng, J, Xue, F. So, Jianmin Shi, Effects of triplet energies and transporting properties of carrier transporting materials on blue phosphorescent organic light emitting devices, Appl. Phys. Lett. 93 (2008) 123306.

29. K. Goushi, R. Kwong, J.J. Brown, H. Sasabe. C. Adachi, Triplet exciton confinement and unconfinement by adjacent hole-transport layers, J. Appl. Phys. 95 (2004), 7798.

30. Y. Kawamura, K. Goushi, J. Brooks, J.J. Brown, H. Sasabe, C. Adachi, 100% phosphorescence quantum efficiency of Ir(III) complexes in organic semiconductor films, Appl. Phys. Lett. 86 (2005), 071104.

31. J. Frischeisen, D. Yokoyama, C. Adachi, W. Brütting, Determination of molecular dipole orientation in doped fluorescent organic thin films by photoluminescence measurements, Appl. Phys. Lett. 96 (2010) 073302.

32. M. Flämmich, M.C. Gather, N. Danz, D. Michaelis, A.H. Bräuer, K. Meerholz, A. Tünnermann, Orientation of emissive dipoles in OLEDs: Quantitative in situ analysis, Org. Electron. 11 (2010) 1039-1046.

33. M. Flämmich, D. Michaelis, N. Danz, Accessing OLED emitter properties by radiation pattern analysis, Org. Electron. 12 (2011) 83-91.

34. W. Brütting, J. Frischeisen, T.D. Schmidt, B.J. Scholz, C. Mayr, Device efficiency of organic light-emitting diodes: Progress by improved light outcoupling, Phys. Status Solidi A 210 (2012) 44-65.

35. D. Yokoyama, C. Adachi, In situ real-time spectroscopic ellipsometry measurement for the investigation of molecular orientation in organic amorphous multilayer structures, J. Appl. Phys. 107 (2010), 123512.

36. D. Yokoyama, Molecular Orientation in small-molecule organic light-emitting diodes, J. Mater. Chem. 21 (2011), 19187.

37. S.S. Dalal, Z. Fakhraai, M.D. Ediger, High-Throughput Ellipsometric Characterization of Vapor-Deposited Indomethacin Glasses, J. Phys. Chem. B 117 (49) (2013) 15415-15425.

38. C. Mayr, S.Y. Lee, T.D. Schmidt, T. Yasuda, C. Adachi, W. Brütting, Efficiency Enhancement of Organic Light-Emitting Diodes Incorporating a Highly Oriented Thermally Activated Delayed Fluorescence Emitter, Adv. Funct. Mater. (2014) doi: 10.1002/adfm.201400495.

39. M.A. Baldo, C. Adachi, S.R. Forrest, Transient analysis of organic electrophosphorescence. II. Transient analysis of triplet-triplet annihilation, Phys. Rev. B 62 (2000) 10967.

40. S. Reineke, K. Walzer, K. Leo, Triplet-exciton quenching in organic phosphorescent light-emitting diodes with Ir-based emitters, Phys. Rev. B 75 (2007) 125328.

41. T.D. Schmidt, D.S. Setz, M. Flämmich, J. Frischeisen, D. Michaelis, B.C. Krummacher, N. Danz, W. Brütting, Evidence for non-isotropic emitter orientation in a red phosphorescent organic light-emitting diode and its implications for determining the emitter's radiative quantum efficiency, Appl. Phys. Lett. 99 (2011), 163302.

42. J.D. Shore, Comment on "Change of the emission spectra in organic light.emitting diodes by layer thickness modification", Appl. Phys. Lett. 86 (2005), 186101.

Figures

Figure 1

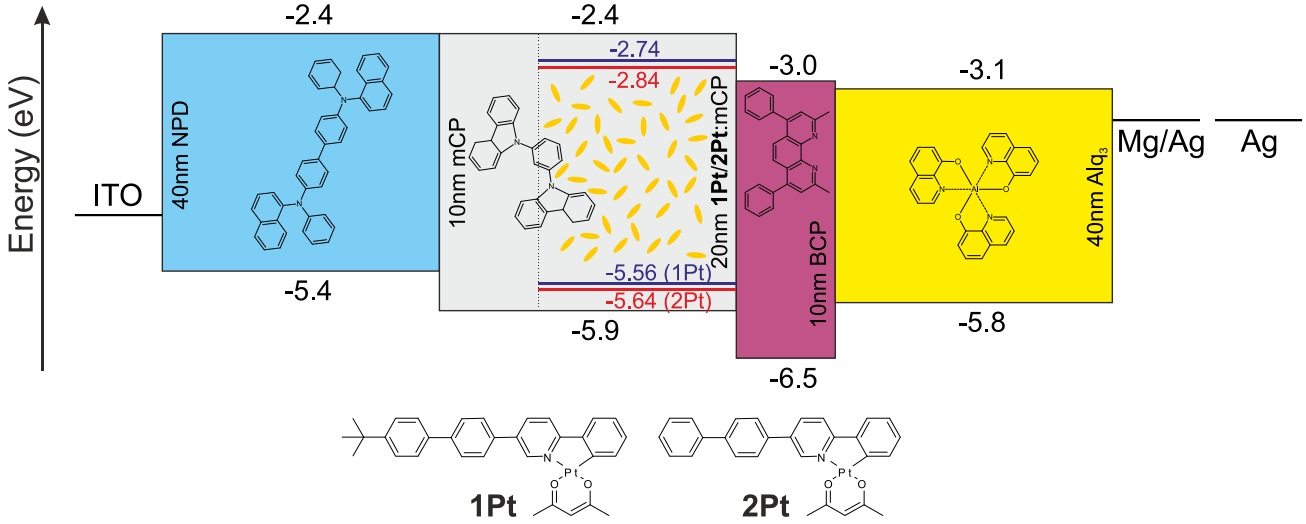

Fig. 1. Energy level diagram, molecular structure of the used materials and stack layout of the investigated OLED devices. The emission layer consists of the Pt(II) complex **1Pt** or **2Pt** doped in mCP (6 wt.%).

C. Mayr et al.

Figure 2

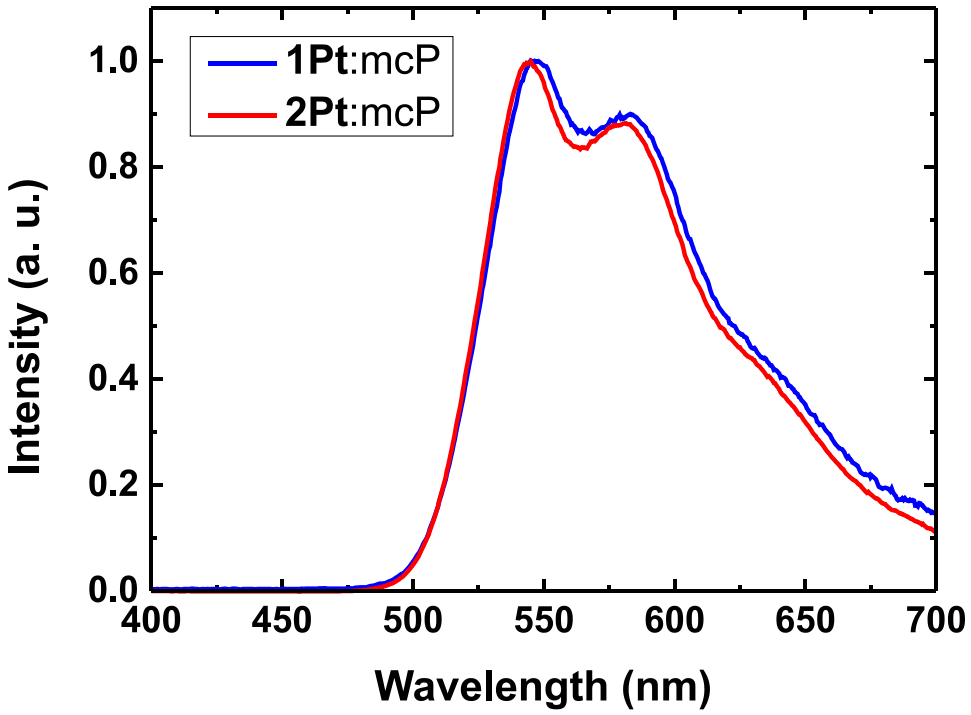

Fig. 2. Photoluminescence emission spectra of 50 nm films of mCP doped with **1Pt** and **2Pt** (6 wt.%) on fused silica substrates.

C. Mayr et al.

Figure 3

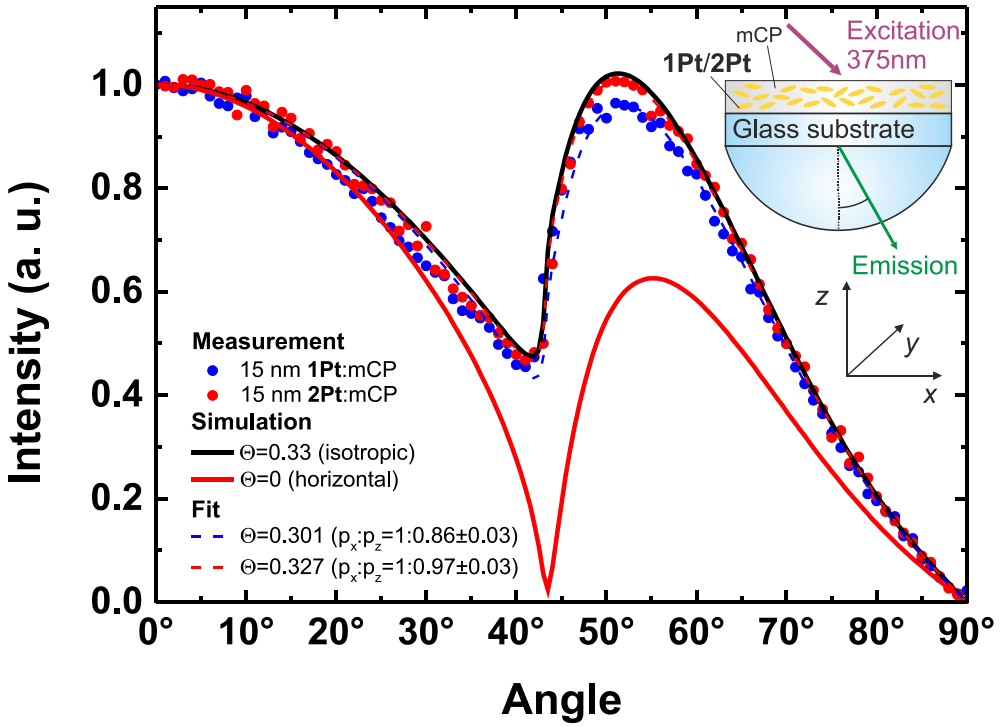

Fig. 3. Cross sections at a wavelength of 580 nm of the measurements and simulations of the angular dependent p-polarized PL emission spectra (considering an emission in the *x*-*z*-plane) for films of 15 nm mCP doped with **1Pt** or **2Pt** (6 wt.%) on glass substrates. The black and the red curve represent the simulations for perfect isotropic (Θ=0.33) and horizontal (Θ=0) orientation of the transition dipole moments, respectively. The measured data have been fitted (dashed lines) for **1Pt** to a slightly more horizontal orientation with Θ=0.301 (p_x:p_z=1:0.86±0.03) and for **2Pt** to an almost isotropic orientation Θ=0.327 (p_x:p_z=1:0.97±0.03).

C. Mayr et al.

Figure 4

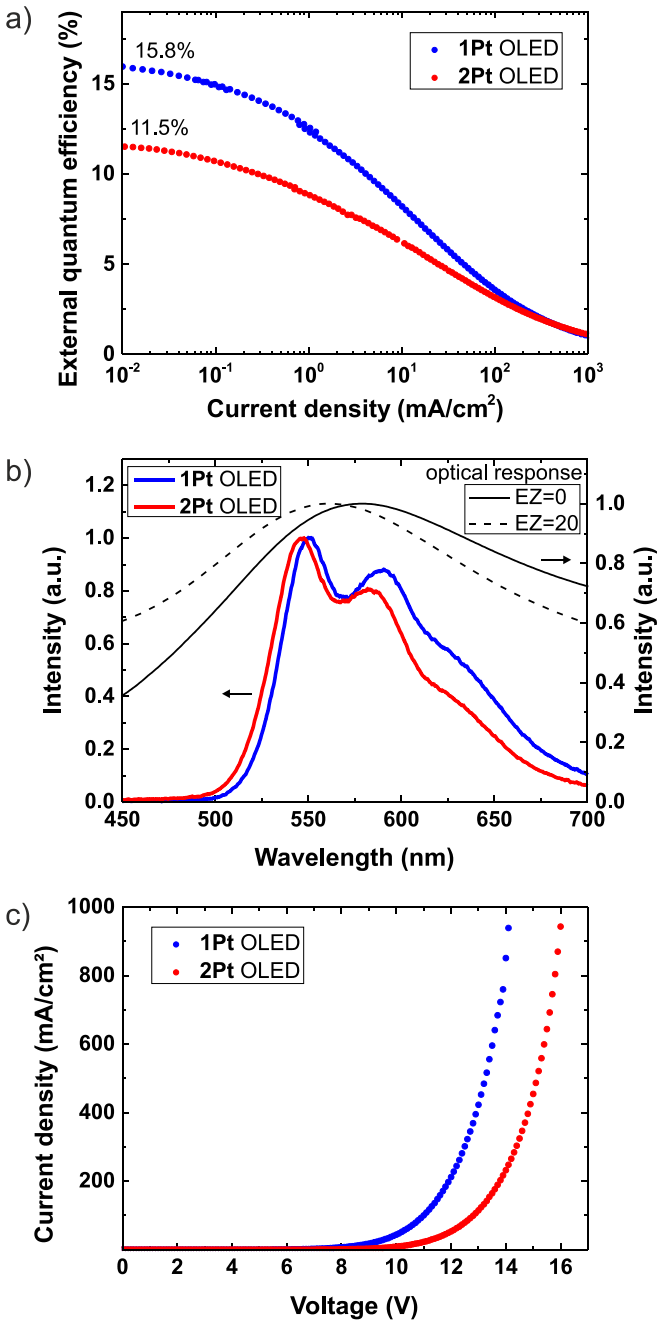

Fig. 4. (a) Measured external quantum efficiency η_{EQE}, (b) normalized EL spectra (peak emission at 550nm for **1Pt** and 546nm for **2Pt**) and optical response for the emission zone located at the interface to the undoped mCP layer (EZ=0) and to the BCP layer (EZ=20), respectively, and (c) current-voltage characteristics for the OLED with either **1Pt** or **2Pt** as the emitter.

C. Mayr et al.

Figure 5

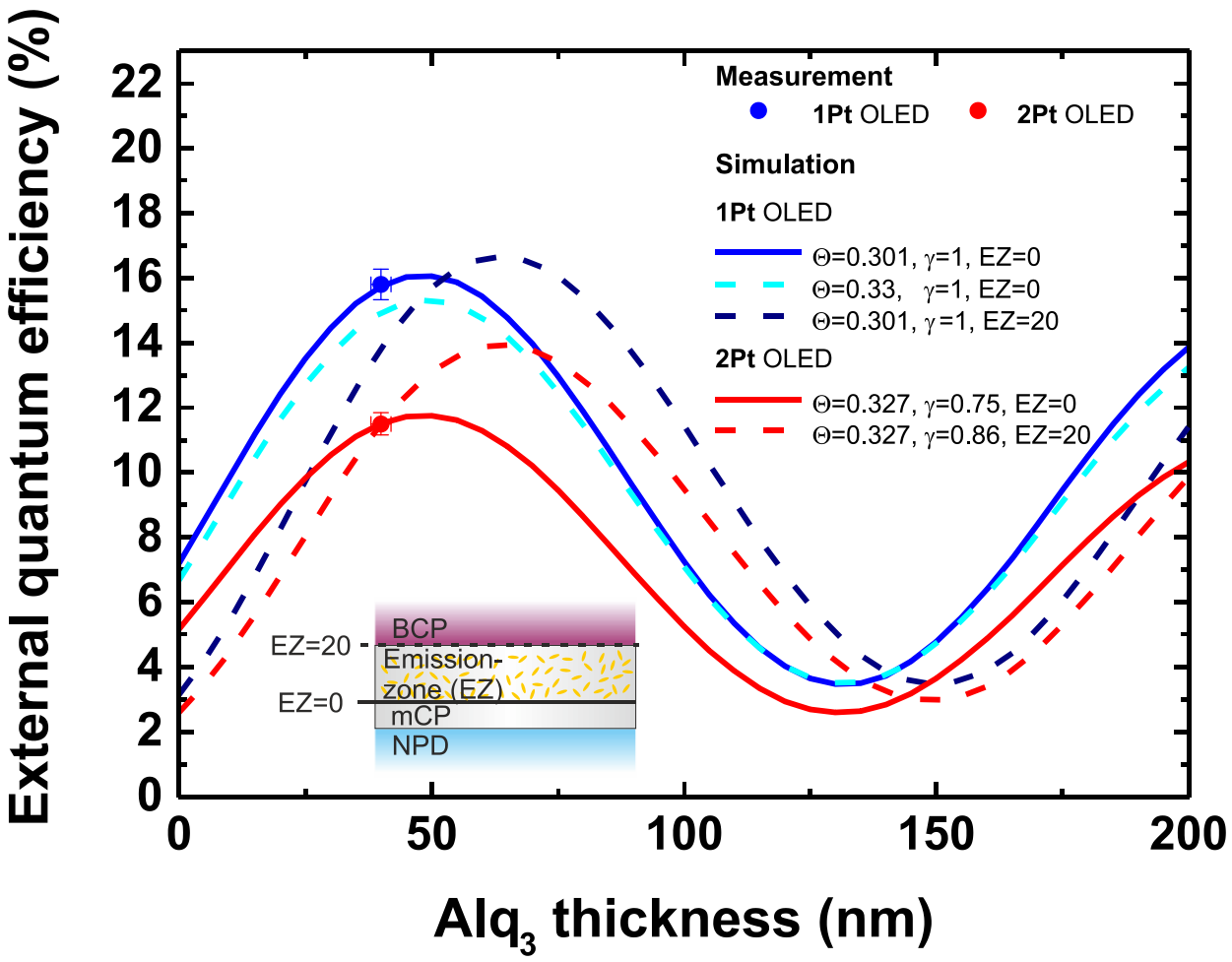

Fig. 5. Calculated η_{EQE} of the OLEDs for varying ETL thickness. For the OLED with **1Pt** as the emitter the simulation fits the measured η_{EQE} by locating the emission zone at the mCP/**1Pt**:mCP-interface (EZ=0) and assuming a non-isotropic orientation of the transition dipole moments (blue solid curve). For the OLED with **2Pt** as the emitter the simulation fits the measured η_{EQE} by assuming an imperfect charge carrier balance. By a possible shift of the emission zone between EZ=0 (red solid line) and EZ=20 (red dashed line), the charge carrier balance can be determined to be 75%<¥ < 86%.

C. Mayr et al.

Figure 6

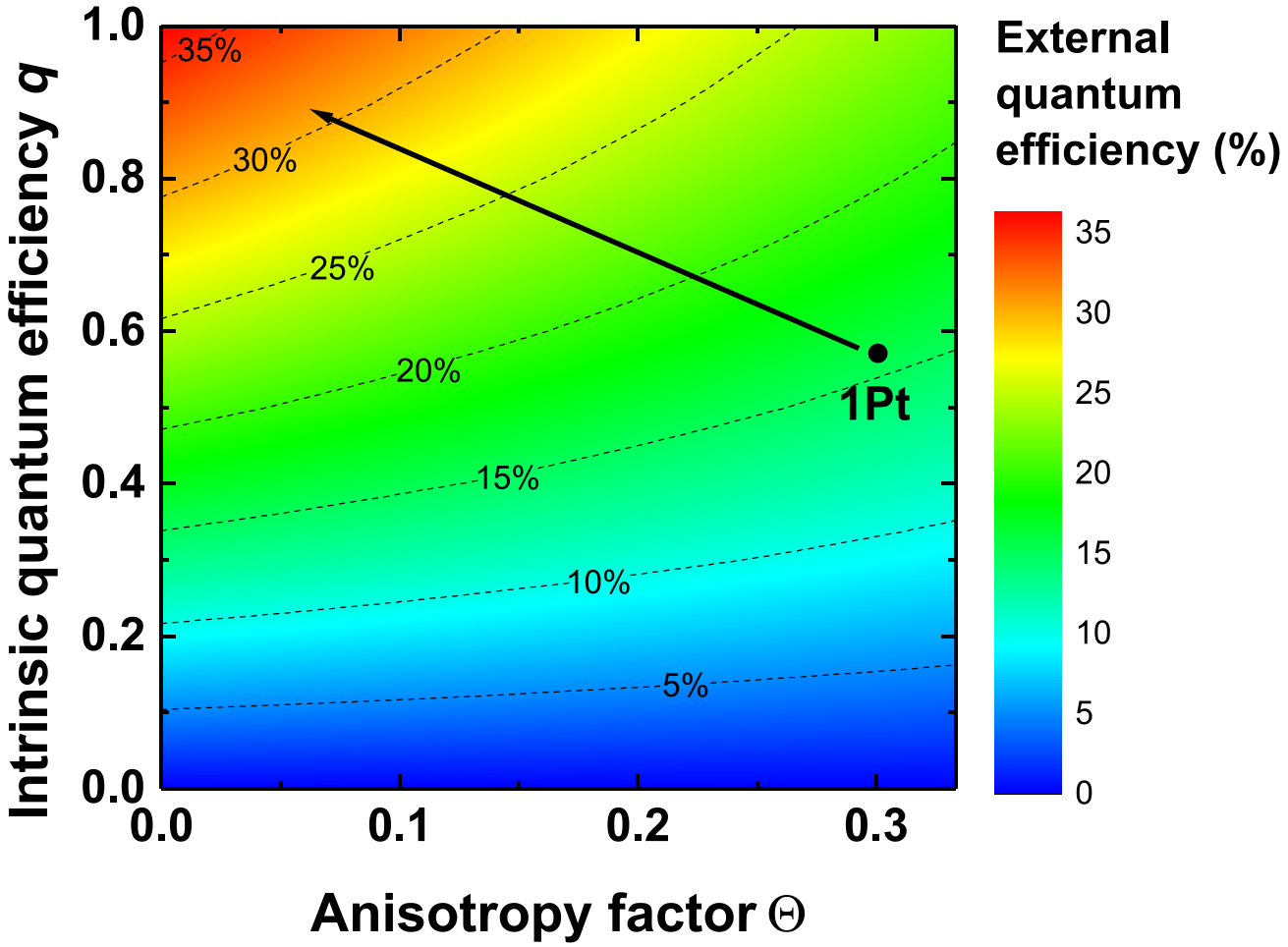

Fig. 6. Calculation of η_{EQE} for the OLED with the device structure shown in Fig. 1 for a varying intrinsic quantum efficiency q and orientation of the transition dipole moments. A radiative exciton fraction and a charge carrier balance of 100% were assumed. By increasing the horizontal orientation of the transition dipole moments and intrinsic quantum efficiency of the emitter η_{EQE} of 36.3% is possible without the use of outcoupling structures.

Tables

Table 1

Dopant	*Orientation*	*Charge carrier balance* ¥	*Radiative exciton fraction* ¦ $_r$	*Effective quantum efficiency* q_{eff}	*Outcoupling efficiency* ¦ $_{out}$	*Calculated* ¦ $_{EQE}$ *(measured) (%)*
1Pt	Θ=0.301	1	1	0.664	0.237	15.7 (15.8)
	Θ=0.33	1	1	0.665	0.225	14.9
	Θ=0	1	1	0.648	0.363	23.5
2Pt	Θ=0.327	0.75< ¥ < 0.86	1	0.672	0.228	11.5 (11.5)

Table 1. Calculated and measured ¦ $_{EQE}$ for the OLED comprising either **1Pt** or **2Pt** as the emitter. Different degrees of orientation of the transition dipole moments have been taken into account for the calculation of the effective quantum efficiency (due to different cavity effects) and outcoupling efficiency.

C. Mayr et al.

Supplementary Information

S1. Material synthesis

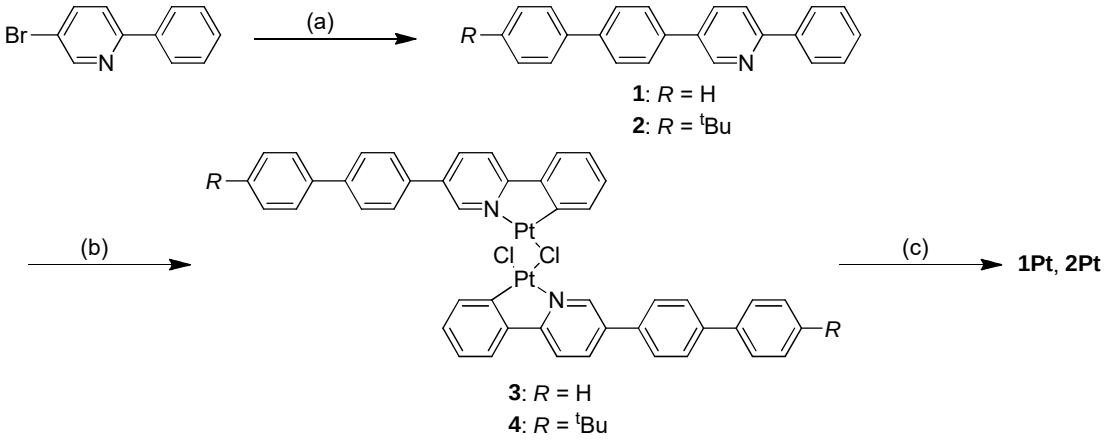

Scheme S1. Synthesis of linear-shaped platinum(II) complexes; (a) arylboronic ester, potassium carbonate, Tetrakis(triphenylphosphine)palladium(0), THF, H_2O, 60 ˚C; (b) potassium tetrachloroplatinum(II), acetic acid, 100 °C; (c) potassium carbonate, 2-ethoxyethanol, 100 °C, 10 h.

Synthesis of ligand 1

5-bromo-2-phenylpyridine (0.585 g, 2.5 mmol), 2-(4-Biphenylyl)-4,4,5,5-tetramethyl-1,3,2-dioxaborolane (0.840 g, 2.5 mmol), K_2CO_3 (4.15 g, 30 mmol), $Pd(PPh_3)_4$ (0.580 g, 0.50 mmol), degassed THF (60 ml), H_2O (15 ml) were added into a 200 ml three neck round bottom flask with stir bar and condenser. The mixture was heated to 60 ˚C under N_2 for 20 hours. After the solution was cooled to room temperature, THF was evaporated in vacuo and the aqueous layer was extracted with dichloromethane. The organic layer was dried with $MgSO_4$, concentrated, and the residue was purified by column chromatography on silica (mixture of *n*-hexane and dichloromethane was eluent) to produce the desired ligand **3** (0.661 g, 2.15 mmol, 86%).

^{1}H NMR (500 MHz, $CDCl_3$): ¢ = 7.39 (t, *J* = 7.4 Hz, 1H; ArH), 7.43-7.52 (m, 5H; ArH), 7.66 (dd, *J* = 8.4 Hz, *J* = 1.2 Hz, 2H; ArH), 7.72-7.74 (m, 4H; ArH), 7.84 (dd, *J* = 8.2 Hz, *J* = 0.6 Hz, 1H; ArH), 8.06-8.07 (m, 2H; ArH), 9.00 (d, *J* = 1.7 Hz, 1H; ArH). Anal. Calcd for $C_{23}H_{17}N$: C, 89.87; H, 5.57; N, 4.56%. Found: C, 89.85; H, 5.52; N, 4.54%.

Synthesis of ligand 2

The procedure was almost the same as brominated intermediate **1** (yield 84%). 2-(4-(4'-tertbutylbiphenyl)yl)-4,4,5,5-tetramethyl-1,3,2-dioxaborolane was used as a boronic ester instead of 2-(4-biphenylyl)-4,4,5,5-tetramethyl-1,3,2-dioxaborolane.

^{1}H NMR (500 MHz, $CDCl_3$): ¢ = 1.38 (s, 9H, $C\underline{H}_3$), 7.44 (t, *J* = 7.2 Hz, 1H; ArH), 7.50-7.52 (m, 4H; ArH), 7.61 (d, *J* = 7.9 Hz, 2H; ArH), 7.71-7.74 (m, 4H; ArH), 7.84 (d, *J* = 8.2 Hz, 1H; ArH), 8.01 (d, *J* = 8.2 Hz, 1H; ArH), 8.06 (d, *J* = 7.4 Hz, 2H; ArH), 8.99 (s, 1H; ArH). Anal. Calcd for $C_{27}H_{25}N$: C, 89.21; H, 6.93; N, 3.85%. Found: C, 89.26; H, 6.93; N, 3.87%.

Synthesis of platinum(II) «-dichloro-bridged dimer 3

Ligand **1** (0.396 g, 1.3 mmol), potassium tetrachloroplatinum(II) (0.535 g, 1.3 mmol), H_2O (4 ml) and acetic acid (20 ml) were added into the three neck round bottom flask with stir bar and condenser. The mixture was heated to 100 ˚C for 12 hours under Ar. After the mixture was cooled to room temperature, the mixture was filtrated followed by washing with water and methanol. The obtained solid (0.615 g, 0.57 mmol, 89%) was desired dimers and used in the next step without further purification.

Synthesis of platinum(II) «-dichloro-bridged dimer 4

The procedure was almost same as dimer **3** (yield 71%). Ligand **2** was used instead of ligand **1**.

Synthesis of 1Pt

Dimer **3** (0.615 g, 0.57 mmol), potassium carbonate (0.790 g, 5.7 mmol), acetylacetone (0.310 g, 3.1 mmol), and 2-ethoxyethanol (30 ml) were added into the three neck round bottom flask with stir bar and condenser. The mixture was heated to 100 ˚C for 10 hours under Ar. After the mixture was cooled to room temperature, the mixture was filtrated followed by washing with hexane. Recrystallization of the obtained residue from THF gave a crude complex. Further purification by recrystallization from dichloromethane/*n*-hexane gave a pure complex **1Pt** (0.291 g, 0.48 mmol, 43%).

^{1}H NMR (500 MHz, $CDCl_3$): ¢ = 2.02 (s, 6H; CH_3), 5.49 (s, 1H; CH), 7.12 (dt, *J* = 7.5 Hz, *J* = 1.2 Hz, 1H; ArH), 7.22 (dt, *J* = 7.4 Hz, *J* = 1.3 Hz, 1H; ArH), 7.39 (t, *J* = 7.3 Hz, 1H; ArH), 7.47-7.50 (m, 8H; ArH), 8.06 (dd, *J* = 8.3 Hz, *J* = 2.1 Hz, 1H; ArH), 9.31 (d, *J* = 2.1 Hz, 1H; ArH). Anal. Calcd for $C_{28}H_{23}NO_2Pt$: C, 56.00; H, 3.86; N, 2.33%. Found: C, 55.92; H, 3.84; N, 2.33%.

Synthesis of 2Pt

The procedure was almost the same as for complex **1Pt** (yield 65%). Dimer **4** was used instead of dimer **3**.

^{1}H NMR (500 MHz, $CDCl_3$): ¢ = 1.41 (s, 9H; CH3), 2.05 (s, 6H; CH_3), 5.52(s, 1H; CH), 7.15 (t, *J* = 7.5 Hz, 1H; ArH), 7.25 (t, *J* = 6.9 Hz, 1H; ArH), 7.50-7.54 (m, 3H; ArH), 7.62-7.78 (m, 11H; ArH), 8.08 (dd, *J* = 8.5 Hz, *J* = 2.0 Hz, 1H; ArH), 9.33 (d, *J* = 2.0 Hz, 1H; ArH). Anal. Calcd for $C_{32}H_{31}NO_2Pt$: C, 58.53; H, 4.76; N, 2.13%. Found: C, 58.47; H, 4.77; N, 2.12%.

S2. Angular dependent PL-emission spectra

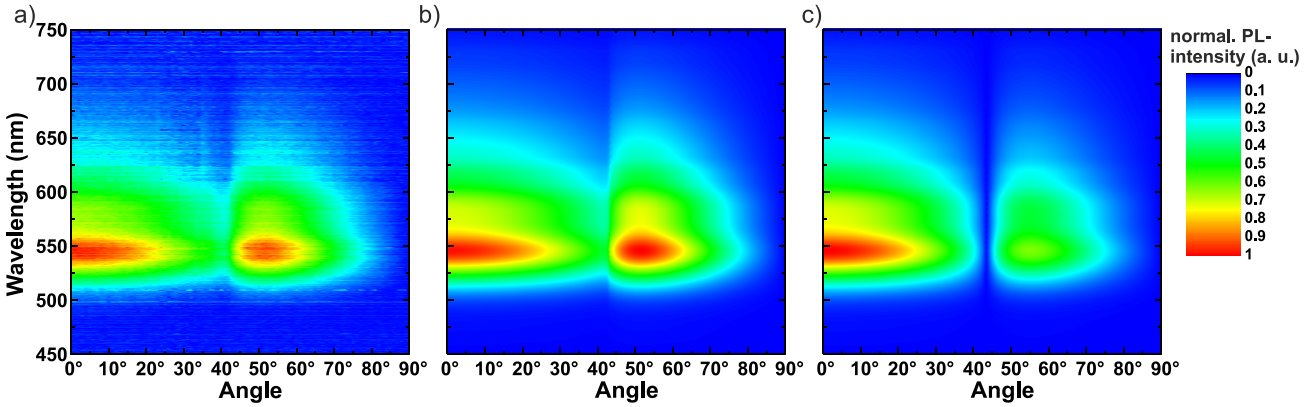

Fig S.1. P-polarized angular dependent PL-emission spectra for films of 15 nm mCP doped with doped with **1Pt** on a glass substrate: a) Measurement, b) simulation for perfect isotropic (Θ=0.33) and c) perfect horizontal (Θ=0) orientation of the transition dipole moments.

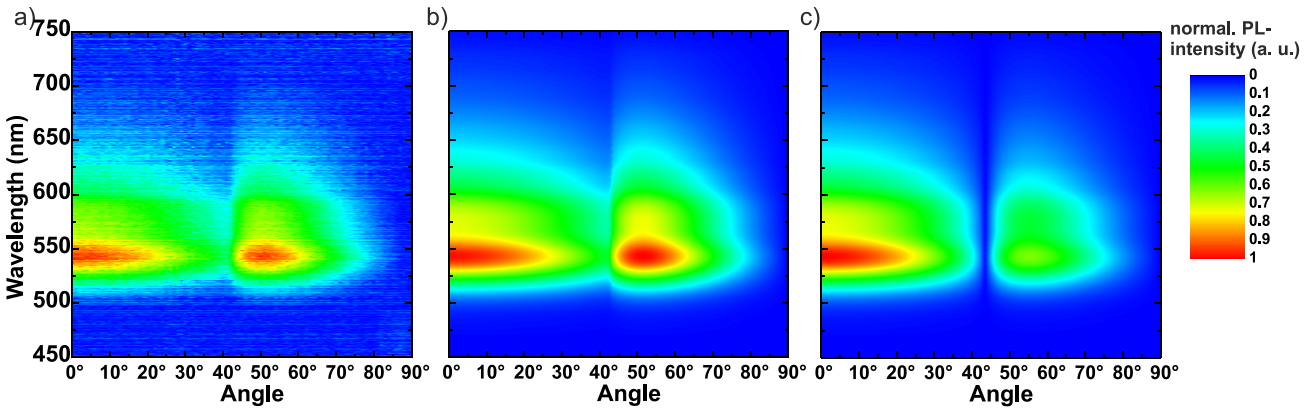

Fig S.2. P-polarized angular dependent PL-emission spectra for films of 15 nm mCP doped with doped with **2Pt** on a glass substrate: a) Measurement, b) simulation for perfect isotropic (Θ=0.33) and c) perfect horizontal (Θ=0) orientation of the transition dipole moments.